Journal of Magnetism and Magnetic Materials 475 (2019) 787–793

Contents lists available at ScienceDirect

Journal of Magnetism and Magnetic Materials

journal homepage: www.elsevier.com/locate/jmmm

Research articles

DNA engineered magnetically tuned cobalt ferrite for hyperthermia application

Arpita Das[a,*], Debarati De[a], Ajay Ghosh[a], Madhuri Mandal Goswami[b,*]

[a] CRNN, University of Calcutta, Kolkata 700098, India
[b] S.N. Bose National Centre for Basic Science, Kolkata 700098, India

ARTICLE INFO

Keywords:
DNA engineered Co-ferrite
Magnetic nanoparticles (MNPs)
Hyperthermia therapy

ABSTRACT

In this work, we report that tuning of magnetic properties of cobalt ferrite magnetic nanoparticles (CFMNPs) is possible by combining them with some suitable organic molecules like DNA for hyperthermia therapy. Different batches of CFMNPs were synthesized on DNA scaffold (with varying the DNA concentrations for different batches) by wet chemical co-precipitation method. Final product was characterized by Fourier transform infrared spectroscopy (FT-IR), Scanning electron microscope (SEM) for biological samples, Transmission electron microscope (TEM), Superconducting quantum interference device (SQUID), X-ray diffraction (XRD), Isothermal Titration Calorimetry (ITC) etc. From XRD data it was confirmed that the above mentioned nanoparticles are cobalt ferrite in pure phase and from FT-IR, SEM and TEM analyses, it was observed that cobalt ferrite nanoparticles were properly attached with DNA. Changes in magnetic properties with change of DNA amount for different batches were investigated by SQUID magnetometer. Heating ability under alternating current (AC) magnetic field for different batches of particles was investigated. It was observed that heating property was changing with change in DNA concentration. So it can be concluded that we have synthesized particles where DNA plays a very important role in tuning the magnetic properties which may give us opportunity to customize the particles for hyperthermia therapy.

1. Introduction

There has been a huge increase in the use of magnetic nanoparticles (MNP) in the application of biomedical field, in recent years. In biomedical uses apart from the biocompatibility, another important criteria for MNPs is their magnetic properties. On the basis of versatility of magnetic properties, MNPs shows different promising applications like targeted drug delivery, magnetic resonance imaging and magnetic fluid hyperthermia etc [1]. Magnetic hyperthermia received enormous attention for its highly promising therapeutic application due to its less adverse side effect than other treatments. This method involves two stages, first delivering the MNPs selectively to the targeting region like tumor and second placing of tumor suitably under an (AC) induced magnetic field [2–4]. Magnetic hyperthermia is a therapeutic procedure where a dispersion containing magnetic nano particles is injected into a tumor containing cancerous cells and if an alternating magnetic field is applied on the tumor it causes a temperature rise of the MNPs (due to relaxation losses of the dispersed magnetic nanoparticles) ultimately leading to a rise in tumor temperature thereby aiding in cancer treatment. It has been reported that a rise in cell temperature beyond 42 °C leads to cancerous cell degradation and apoptosis. [5–7]. Thus tumor growth can be arrested. But before placing MNPs inside the tumor, their heating ability should be investigated, in some analogous laboratory test set up. Not only heating capacity, but also their surface properties should be investigated for the selective attachment of the MNP with the tumor. Toxicity is also another very important aspect in case of successful use of the MNPs for hyperthermia therapy. To reduce the toxicity, proper biofunctionalization is also required. So, functionalization of these types of MNPs with proper bio molecule is highly needed. Not only to target the tumor, but also to bind the drug molecule with MNPs for specific drug delivery, proper functionalization is required [8,9]. Sometimes the desired medication doses become much higher which become hazardous for whole body and results in adverse side effects. If the drug incorporated MNPs can be delivered to tumor region without affecting whole body and drug can be released in a controlled manner only in the tumor site by application of AC magnetic field that will be another important achievement in such hyperthermia therapy [10]. So most emphasis should be given to increase the efficiency of heating by engineering the MNPs properly, changing their some of the parameters like internalization MNPs with the cells, magnetic properties etc.

* Corresponding authors.
E-mail addresses: arpitadas166@gmail.com (A. Das), madhuri@bose.res.in (M.M. Goswami).

https://doi.org/10.1016/j.jmmm.2018.11.092
Received 23 June 2018; Received in revised form 9 November 2018; Accepted 18 November 2018
Available online 26 November 2018
0304-8853/

[11,12].

Here we have synthesized different batches of cobalt ferrite magnetic nanoparticles (CFMNPs) on the DNA scaffold with increasing amount of DNA while keeping the amount of cobalt ferrite same. The change of magnetic properties with change of DNA amount is also investigated since heat dissipation by the particles under AC magnetic particles depends on the magnetic property of MNPs and heating efficiency is most important criteria for the MNPs to be used for hyperthermia therapy. Particles are characterized by different techniques to be sure about their structure, phase, size, fictionalization, magnetic properties etc.

2. Experimenal set up

2.1. Synthesis of cobalt ferrite nanoparticles (CFNPs)

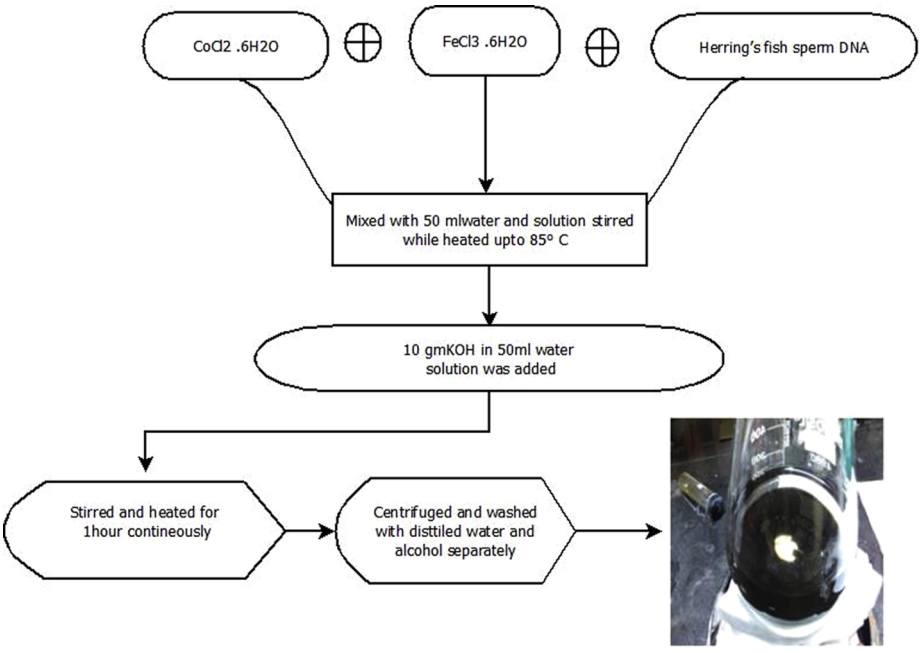

By wet chemical co precipitation method CFNPs were synthesized. At the beginning $FeCl_3{\cdot}6H_2O$ & $CoCl_2{\cdot}6H_2O$ in 1:2 M ratios were dissolved in 50 ml of distilled water. In another beaker 10 gm KOH was dissolved in 50 ml distilled water and kept separately. Different amount of DNA (0.1 g, 0.2 g, 0.4 g & 0.8 g) were taken separately and dissolved in 100 ml of distilled water for each batch. We have prepared 4 batches of samples (Batch 1: CF NPs without DNA labeled as 0.0 DNA, Batch2: CFNPs + 0.2 g DNA labeled as 0.2 DNA batch, Batch3: CFNPs + 0.4 g DNA labeled as 0.4DNA batch and Batch4: CFNPs + 0.8 g DNA labeled as 0.8DNA batch). For batch1 $FeCl_3{\cdot}6H_2O$ & $CoCl_2{\cdot}6H_2O$ in 50 ml water solution & 100 ml additional distilled water were added to make total volume 200 ml. It was then heated & stirred until the temperature reached to 85 °C. Then the KOH solution was added all at time to it and the solution was stirred for 1 h at 85 °C. After 1 h the final product formed was kept in rest at room temperature to settle down the particles. Finally the particles were washed with distilled water and alcohol repeatedly. The precipitate was then dried properly. In case of batch 2, 3 and 4 different amount of DNA like 0.2 g, 0.4 g & 0.8 g were dissolved in 100 ml of distilled water and were added with $FeCl_3$ & $CoCl_2$ solution. After that the same protocol was followed.

2.2. Characterisation of magnetic nanoparticle

2.2.1. Instruments

The X-ray diffraction (XRD) measurement was done by Rigaku Miniflex II desktop X–ray diffractometer under a 2θ range of 20–80 degree using λ = 0.154 nm (Cu-Kα) radiation. To investigate the interaction between cobalt ferrite and DNA, Fourier transformed infra-red (FTIR) was performed on the sample by JASCO FTIR 6300 instrument. BIOSEM (ZEISS EVO-MA 10) and TEM (JEM-2100HR-TEM, JEOL, Japan) images were captured to get morphological information of the MNPs. Magnetic measurements were done in SQUID instrument. Binding of CFMNPs with DNA was confirmed by Isothermal Titration Calorimetry (ITC) method (Malvern Model Microcal ITC 200). A solenoid coil (174 number of turns, 6.14 A applied current, 50 Hz supply frequency) has been made to measure the change in temperature. A

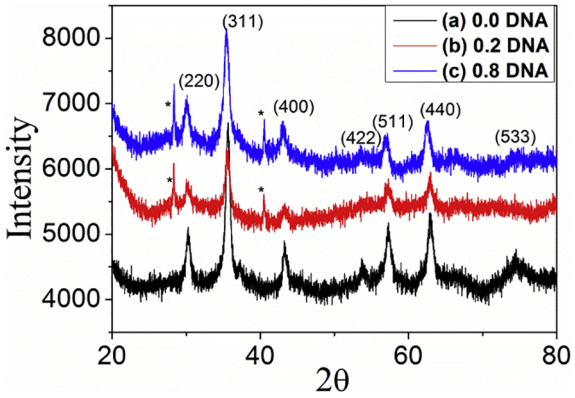

Fig. 1. XRD spectrum (a) only cobalt ferrite without DNA (b) 0.2 g DNA (c) 0.8 g DNA.

Table 1
Calculating of intercellular spacing of only cobalt ferrite(0.0 batch), 0. 2DNA batch, 0.8 DNA batch.

Peaks	0.0 Batch	'd' spacing (nm)	Peaks	0.2 Batch	'd' spacing (nm)	Peaks	0.8 Batch	'd' spacing (nm)
Peak1 (2,2,0)	X = 30.3532 Y = 7083.4447	d_1 = 0.2945	Peak1 (2,2,0)	X = 28.4958 Y = 5027.4515	d_1 = 0.3132	Peak1 (2,2,0)	X = 28.4959 Y = 6239.9617	d_1 = 0.3132
Peak2 (3,1,1)	X = 35.5343 Y = 8706.3643	d_2 = 0.2563	Peak2 (2,2,0)	X = 30.1577 Y = 4806.2005	d_2 = 0.2963	Peak2 (2,2,0)	X = 30.1577 Y = 6112.2644	d_2 = 0.2783
Peak3 (4,0,0)	X = 43.4037 Y = 6689.9071	d_3 = 0.2084	Peak3 (3,1,1)	X = 35.5343 Y = 5278.2026	d_3 = 0.2526	Peak3 (3,1,1)	X = 35.5343 Y = 7105.2991	d_3 = 0.2526
Peak4 (4,2,2)	X = 53.9613 Y = 6700.3550	d_4 = 0.1699	Peak4 (4,0,0)	X = 40.7153 Y = 5278.2026	d_4 = 0.2216	Peak4 (4,0,0)	X = 40.4954 Y = 5705.1352	d_4 = 0.2227
Peak5 (5,1,1)	X = 57.8056 Y = 7074.1600	d_5 = 0.1603	Peak5 (4,0,0)	X = 43.4036 Y = 4458.7544	d_5 = 0.2084	Peak5 (4,0,0)	X = 42.9882 Y = 5705.1352	d_5 = 0.2103
Peak6 (4,4,0)	X = 63.0771 Y = 7142.6522	d_6 = 0.1473	Peak6 (5,5,1)	X = 57.4805 Y = 4847.1729	d_6 = 0.1473	Peak6 (5,1,1)	X = 57.0650 Y = 5539.8798	d_6 = 0.1613
			Peak7 (4,4,0)	X = 63.0770 Y = 4916.0065	d_7 = 0.1603	Peak7 (4,4,0)	X = 62.6616 Y = 5693.1166	d_7 = 0.1482

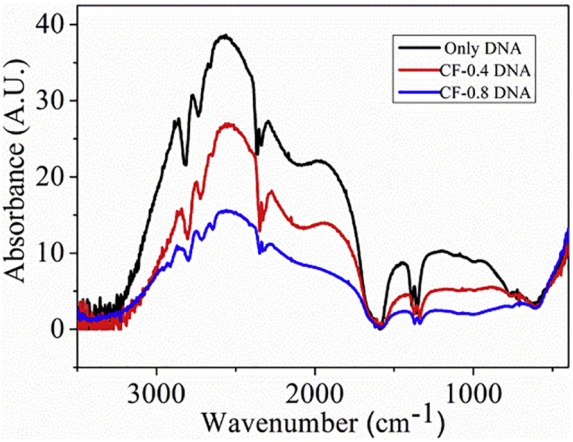

Fig. 2. FT-IR spectrm (a) only Kbr (b) only DNA, (c) only cobalt ferrite, (d) 0.2 g DNA added Cobalt Ferrite. (e) 0.4 g DNA added Cobalt Ferrite (f) 0.8 g DNA added Cobalt Ferrite.

digital thermometer (Hicks) is used to measure the temperature.

2.2.2. Experiments

2.2.2.1. ITC analysis. To check the binding of CFMNPs with DNA, the particles after synthesis were analyzed by ITC method at two different temperatures 37 and 45 °C with varying molar ratio. ITC was performed at both the temperature since the normal body temperature is 37 °C and hyperthermia therapy temperature is 45 °C. Whether DNA remains bound with CFMNPs at both this temperatures that was investigated by this method.

2.2.2.2. AC magnetic field induced heating. To measure the heat, induced in the particle while the MNPs are in hyperthermic condition, we have prepared a basic solenoid with 174 no of turns operating at 230 V with 50 Hz AC supply. From every single batches 1 mg sample were dissolved in 2.5 ml PBS solution and each individual batches were kept in 2 ml plate. We kept another 2 ml plate containing 2.5 ml of PBS only. All of the plates (with and without particles) were kept at a time inside the solenoid with applied current. Then the temperatures were noted at different intervals with the digital thermometer.

2.2.2.3. Labeling of particles with (Rhodamine B isothiocyanate) RITC dye. The MNPs were made fluorescent by tagging them with fluorescent dye 'RITC' to track the movement of particles effectively. For labeling of the CFMNPs by RITC, 25 mg of each different batch of CFMNPs were dispersed in 0.1 M $NaHCO_3$ solution and 1 mg of RITC was dissolved in 2 ml of aqueous DMSO (1:1, V/V) and both the solutions were immediately mixed. Then the mixture was stirred for 24 hrs in the dark at room temperature. Finally the RITC tagged samples were separated by centrifugation at 10,000 rpm at 4 °C from the liquid

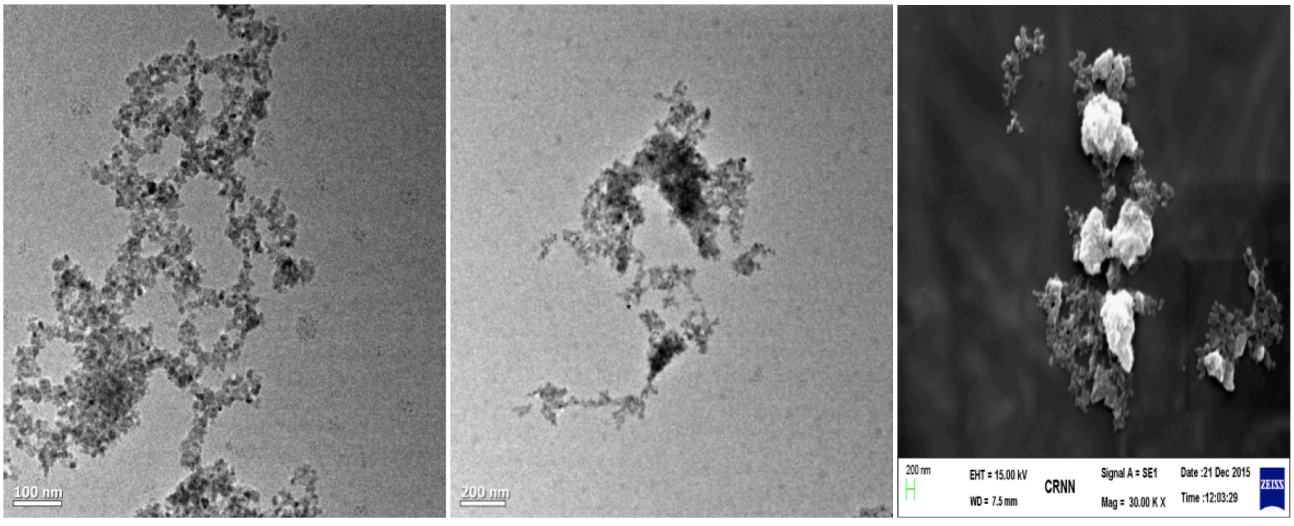

Fig. 3. (a) and (b) TEM and (c) SEM images.

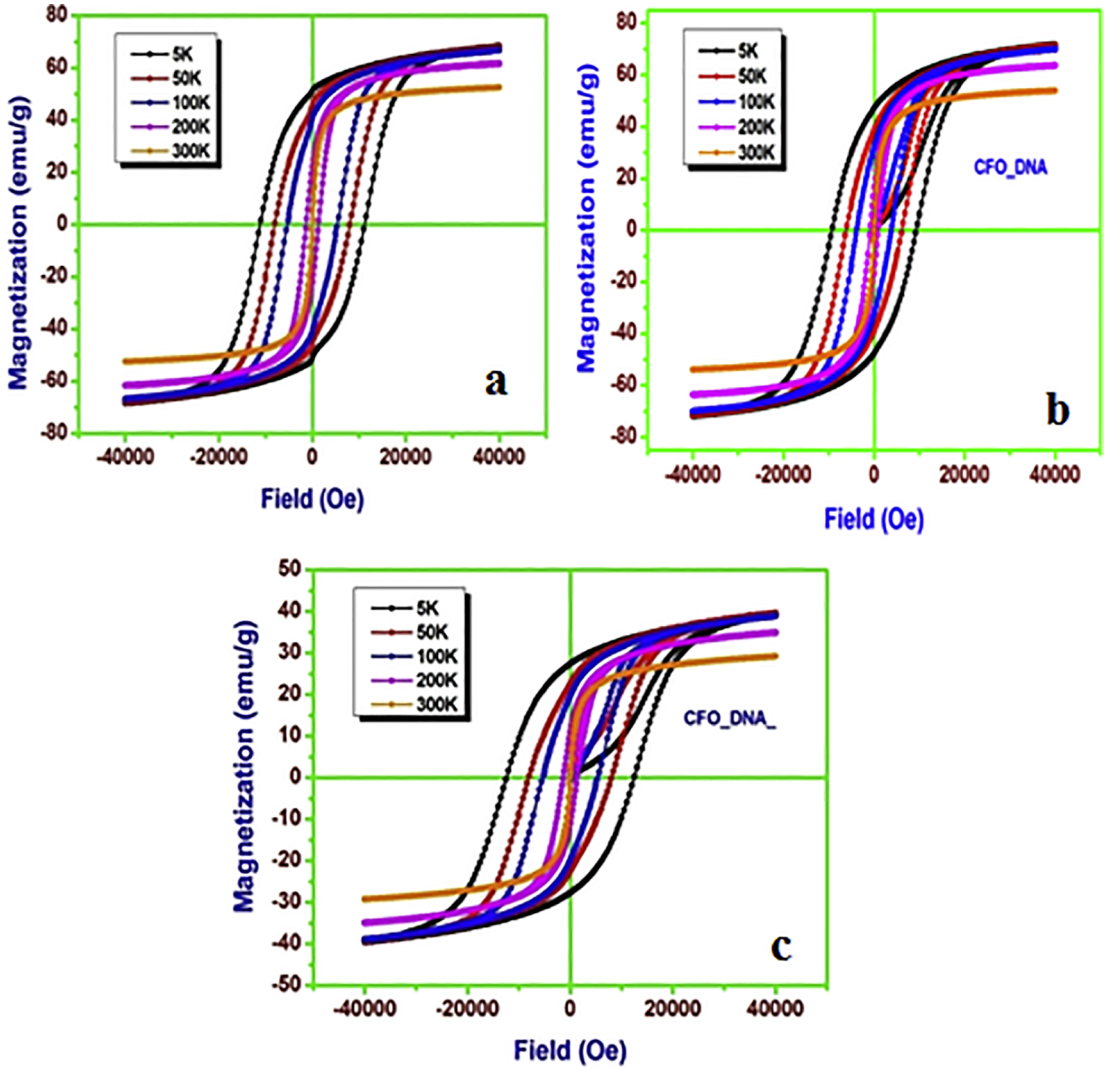

Fig. 4. Magnetic hysteresis loop measurements at different temperatures (a) cobalt ferrite, (b) 0.2 g DNA added CF-NPs, (c) 0.8 g DNA added Cobalt ferrite.

Table 2
Hc measurement.

Temp(K)	Hc (oersted)		
	0.0 DNA	0.2 DNA	0.8 DNA
5 K	12,477	11,217	9363
50 k	8188	8056	6184
100 K	5386	5293	3811
200 K	1340	1295	893
300 k	144	140	86

part. Then the samples were washed with water repeatedly to remove excess RITC that is not attached to the particles.

3. Results discussions

3.1. XRD data analysis

XRD measurement was done in the scanning range 2θ = 20–80° for all the batches of the particles. The XRD patterns for CFMNPs are shown in Fig. 1. The peaks are indexed comparing with JCPDS data which reveals that all diffraction peaks matches with JCPDS (Joint Committee on Powder Diffraction Standards) (card no 22-1086) hence the particles are cobalt ferrite. Except the peaks associated to cobalt ferrite, there are also some unwanted peaks present in the graph in Fig. 1(b) and (c). Here we see that with incorporation of DNA in CFMNPs two new peaks are peeping before (2 2 0) and (4 0 0) peaks in each case which is not observed in case of Fig. 1(a). We presume that this is the consequence of incorporation of DNA inside the CFMNPs. Because of incorporation of DNA the crystal structure of CFMNPs is changed to some extent and evolution of some new peaks are taken place in these two cases. Due to incorporation of DNA inside the CFMNPs a change in crystal structure occurs leading to slight elongation from cubic to tetragonal. The shifts of the peaks were noted and according to that, the inter-planer spacing is calculated from the equation $n\lambda = 2d \sin\theta$ to see the difference. By comparing the results of XRD plots of DNA bound CFMNPs and non-bound CFMNPs, we see shift in Bragg's angle and change in 'd' spacing for CFMNP and DNA bound CFMNP. The detail results are tabulated in Table 1. In this table X means 2θ degree and Y means intensity. This result proves strong binding of DNA with the particles.

3.2. FT-IR data analysis

The FT-IR spectra are taken for different batches of CFMNPs bound with DNA and pure DNA in KBr matrix and shown in Fig. 2. The broad

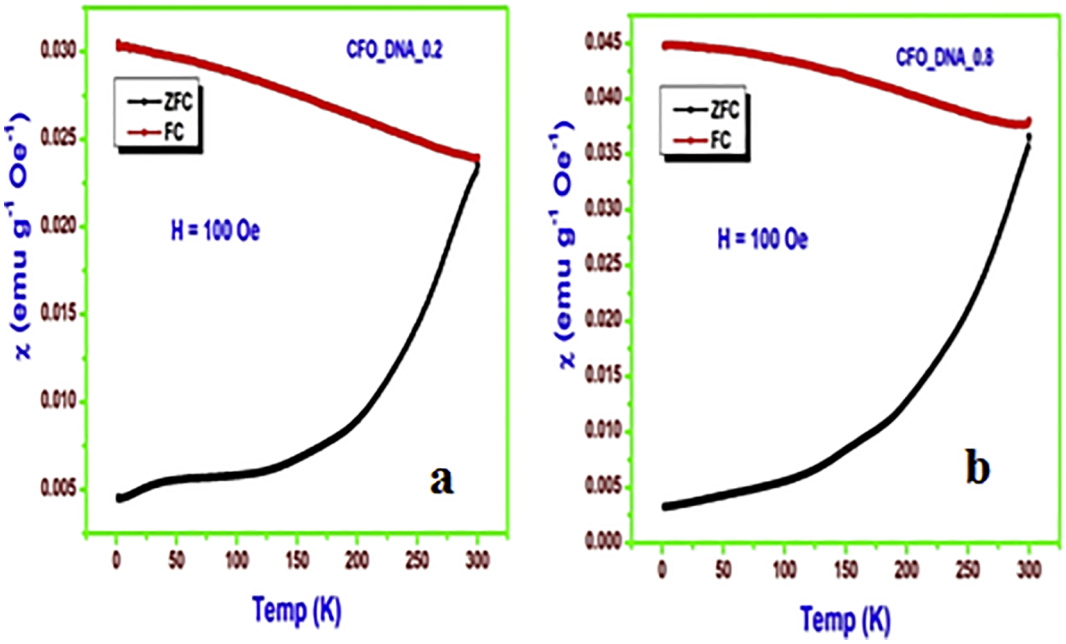

Fig. 5. FC, ZFC curves of 0.2 and 0.8 DNA batch.

Table 3
Heat gain and release by the particle while situating in a solenoid.

Time	Temperature raised (°C) Room temp. 24 °C	Time (actual time of day)	Temperature degraded (°C) Room temp. 26 °C
1 min	26.00	3.23 pm	36
2 min	26.75	3.26 pm(3 min)	34
3 min	27.75	3.29 pm(6 min)	31
4 min	29.00	3.32 pm(9 min)	30
5 min	31.00	3.38 pm(15 min)	29
6 min	32.00	3.42 pm(19 min)	29
7 min	32.50	3.45 pm(24 min)	28
8 min	33.00	3.46 pm(25 min)	28
9 min	34.50	3.50 pm(29 min)	28
10 min	35.00	3.55 pm(34 min)	27
11 min	36.50	3.58 pm(37 min)	26

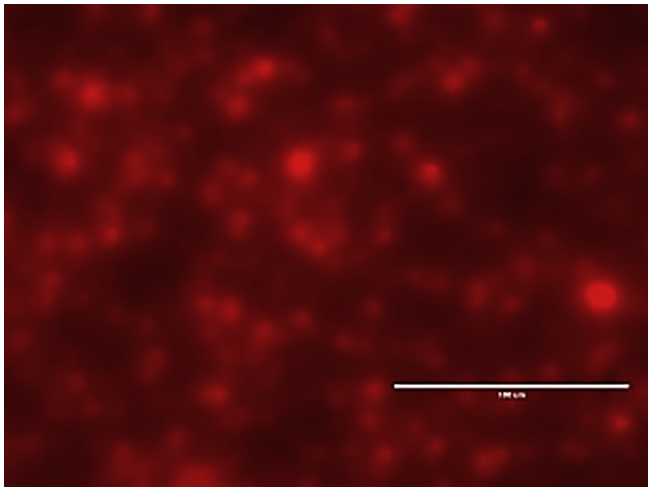

Fig. 6. Fluorescence image of RITC tagged particle.

peak in the range 1324–781 cm^{-1} for pure DNA sample is due to phosphate back bone stretching and bending vibration. The peak in the range 1335–603 cm^{-1} is shifted and become broader due to binding of CFMNPs with DNA. The peak at 1460 cm^{-1} for only DNA and at 1418 cm^{-1} for CFMNP-DNA are due to stretching vibration of COO^{-}.

Comparing all the graphs here we see almost all the peaks coming for only DNA molecules are also coming in case of DNA bound CFMNPs with a shift and broadening which indicates binding of the DNA molecules with the CFMNPs.

3.3. TEM and SEM data analysis

The particles' morphology was analyzed by TEM and SEM (for biological samples) and the images are shown Fig. 3. From TEM results it was fond that the average size of the nano-particles is approximately 13 nm. In the TEM images the organic samples cannot be seen because energy used in TEM measurement is very high so the organic samples burnt out. It is know that the DNA which is attached with the particle is of double helix chain like structure. Here we see a chain like pattern of the particles which is due to sitting of particles on DNA chain. In SEM picture we see white part which is due to presence of DNA.

3.4. DC magnetic data analysis

M – H (magnetic hysteresis) measurement for different matches of particles at different temperatures is done and curves are shown in Fig. 4. Results are tabulated in Table 2. With increase of DNA amount the coercivity value for the DNA bound sample decreases. DNA is diamagnetic in character. Contribution of diamagnetic material in ferromagnetic sample decrease the coercivity in the DNA bound CFMNPs. It

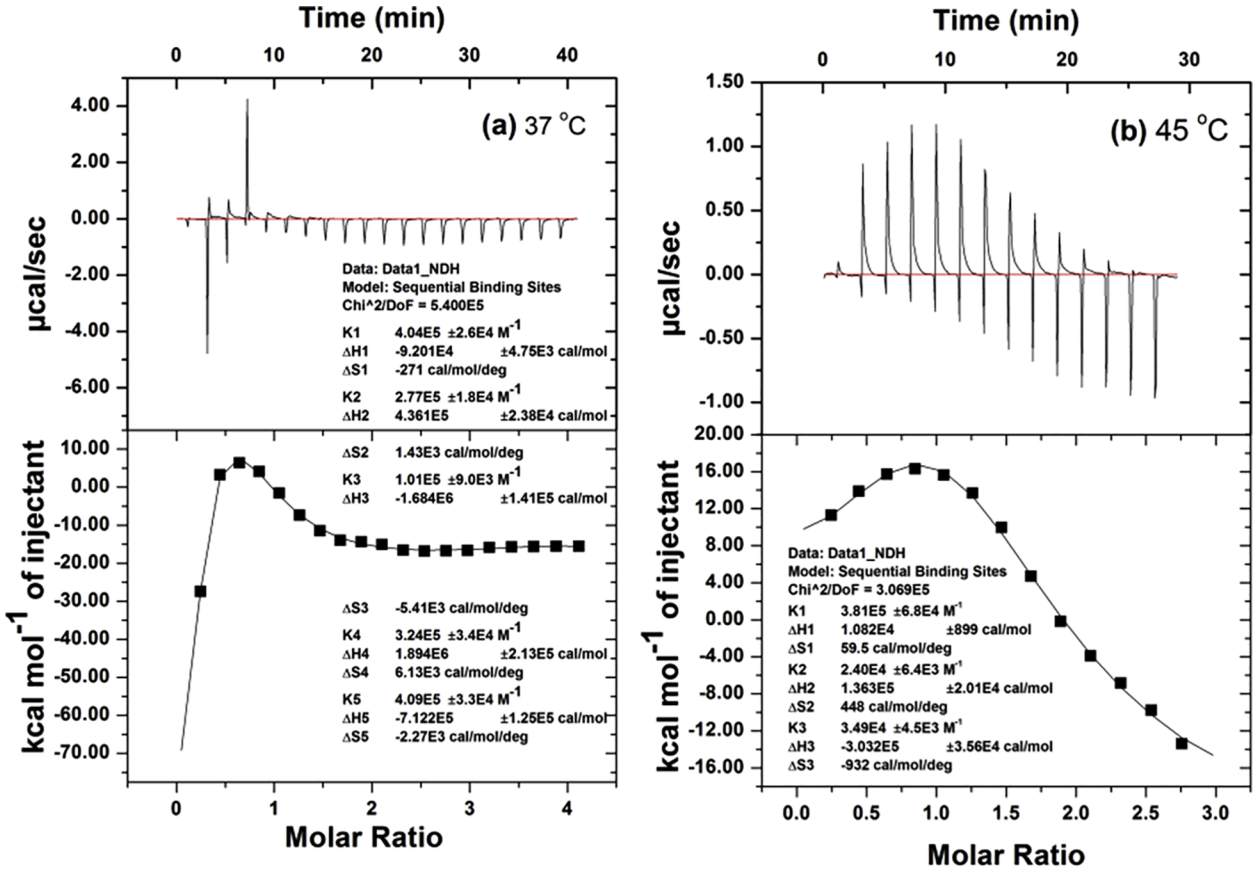

Fig. 7. ITC analysis of DNA added MNP at 45 °C and 37 °C temperature.

can be suggested that the significant decrease in coercivity Hc due to weakening of anisotropy barrier which starts due to thermal agitation [13] The saturation magnetization value here for CFMNPs is comparable with the other published values of cobalt ferrite MNP [14,15]. The saturation value for DNA-CF particles decreases due to diamagnetic contribution coming from DNA molecules. This again conform the binding of DNA to CF. The bonding between the Fe (metal citations) of Cobalt Ferrite with the phosphate back bone of DNA (anions of DNA chain) can affect the anisotropy energy, which will contribute immensely in changing the magnetic property [17].

From the previous research work in this field it has been proved that, whenever micells act as a caping agent with the single domain cobalt ferrite nanoparticls, enhances the coercivity of the particle by large extent. Here micells are helping to induce high coercivity by making a cage like sterically hindered structure, that the formed around the particles, which arrest the spin of the paticle, results the substancial anisotropy of the particle enhances the coercivity [18].

The FC (field cooled) and ZFC (zero field cooled) curves measured at 100 Oe (7977 A/m) applied field are shown in Fig. 5 for two different batches. M-H loop is measured by taking a known amount of solid powdered sample. The ZFC FC measurement has been done to indicate that the ferromagnetic nature of the sample at room temperature and at lower frequency. Generally at lower frequencies, few particles having relaxation time less than the measuring time, and will behave superparamagnetically but most of the particles will behave ferromagnetically when the measuring time is less than the relaxation time of the particles, i.e. at higher frequencies. So, as the frequency of the AC magnetic field increases, the fraction of ferromagnetic particles increases and this phenomenon results higher coercivity at higher frequencies [16]. Hence more the ferromagnetic nature of the sample more the hysteresis loop area in M-H measurement can be developed Both of FC curves shows a gradual decrease of magnetic susceptibility with increasing temperature from 200 K to 300 K and in case of ZFC curves increases gradually and both the ZFC and FC curves will meet after 300Kwhere we can have the blocking temperature. Hence the blocking temperature for these samples is more than 300 k which indicates ferromagnetic nature of the samples.

3.5. Temperature gain measurements in the solenoid

The solenoid induces a magnetic field of around 7.897 mT and inductance 0.729 mH inside the coil. Table 3 shows 4 different columns of tabulation, the first two columns shows the temperature gained by the particle (in the PBS solution) inside the solenoid (with applied current), for particular time intervals. The last two column shows the temperature looses by these same particles (in PBS solution), outside the solenoid for particular time intervals. We can see the particle solution gain heat quickly. But in the other 2 ml plate where only the PBS solution (without particles) the temperature remains constant. And comparatively we can see that, after taking out from the circuit they take little long time to cool down, so it is good for the therapeutic treatment as it will helps us to kill the tumor cells more effectively. AC magnetic field is agitating the ferromagnetic property of these particles, as they starts to fluctuate faster they started to generate more heat which is the main optimum condition for magnetic hyperthermia.

3.6. Fluorescence imaging of the RITC tagged particles

After attaching the RITC dye with particles the fluorescence images were taken which is shown in Fig. 6. From the figure we can see that the particles were successfully functionalized with the RITC dye as we can visualize them in Red Fluorescent region. It will help us to probe the cells or any other organs by attaching these particles to the concerned region.

3.7. ITC data analysis

From Fig. 7(a and b) it is evident that sequential binding of the DNA with the CFMNPs takes place indicating opening of more than 5 sites. In Fig. 7 a we see that first the process was exothermic and after 40 min also the process is not getting perfectly saturated as more sites are getting opened as the process continues. In Fig. 7b we see with increase in temperature the process became completely exothermic from endothermic condition which confirms that at higher temperature which is used as cell killing temperature, the particles are bound to DNA.

4. Conclusion

From all the above discussed results it is observed that the synthesized cobalt ferrite is properly engineered on DNA scaffold. 85 °C temperature is high enough to make the DNA single helix structure, but as the temperature cools down it can further get back to its original form by regenerating the double helix structure. As the DNA molecules are incorporated inside the particles the structural changes in the lattice is visibly seen which confirms the attachment of DNA with the particles. This type of attachment is also verified by the ITC data. The changes in magnetic properties with change of DNA amount will help us to obtain customized particles with suitable magnetic properties for hyperthermia therapy.

Acknowledgements

Authors are thankful to the Department of Science and Technology, Government of India for the funding under the project SR/WOS-A/CS-158/2016 and to S.N. Bose Centre, Kolkata for providing the fund and other facilities. Debarati De is grateful to Department of Science and Technology, Government of India for Inspire fellowship.

References

[1] K.M. Krishnan, IEEE Trans. Magn. 46 (2010) 2523.
[2] J.W. Lagendijk, Phys. Med. Biol. 45 (2000) R61.
[3] A. Jordan, R. Scholz, K. Maier-Hauff, M. Johannsen, P. Wust, J. Nadobny, H. Schirra, H. Schmidt, S. Deger, S. Loening, W. Lanksch, R. Felix, J. Magn. Magn. Mater. 225 (2001) 118.
[4] K. Maier-Hauff, R. Rothe, R. Scholz, U. Gneveckow, P. Wust, B. Thiesen, A. Feussner, A. von Deimling, N. Waldoefner, R.A. Jordan, J. Neurooncol. 81 (2007) 53.
[5] P. Moroz, S.K. Jones, B.N. Gray, Int. J. Hyperthermia 18 (2002) 267.
[6] K. Maier-Hauff, F. Ulrich, D. Nestler, H. Niehoff, P. Wust, B. Thiesen, H. Orawa, A. Jordan, J. Neurooncol. 103 (2011) 317.
[7] M. Johannsen, U. Gneveckow, B. Thiesen, K. Taymoorian, C.H. Cho, N. Waldöfner, R. Scholz, A. Jordan, S.A. Loening, P. Wust, Eur. Urology 52 (2007) 1653.
[8] C.C.P. erstappen, J.J. Heimans, K. Hoekman, TJ. Postma, Neurotoxic complications of chemotherapy in patients with cancer: clinical signs and optimal management, Drugs 63 (2003) 1549–1563.
[9] G.P.K upta, Drug targeting in cancer chemotherapy: a clinical perspective, J. Pharm. Sci. 79 (1990) 949–962.
[10] A. Lubbe, C. Bergemann, J. Brock, D.G. McClure, Physiological aspects in magnetic drug-targeting, J. Magn. Magn. Mater (1999) 149–215.
[11] C.F. Huang, X.Z. Lin, W.H. Lo, in: 2010 Annu. Int. Conf. IEEE Eng. Med. Biol., 2010, pp. 3229–3232.
[12] Tang. I-Ming, Nateetip Krishnamra, Narattaphol Charoenphandhu, Rassmidara Hoonsawat, Weeraphat Pon-On (2011) 6–19.
[13] Chaitali Dey, Kaushik Baishya, Arup Ghosh, Madhuri Mandal Goswami, Ajay Ghosh, Kalyan Mandal, J. Magn. Magn. Mater. 427 (2017) 168–174.
[14] K. Maaz, A. Mumtaz, S.K. Hasanain, A. Ceylan, J. Magn. Magn. Mater. 308 (2007) 289–295.
[15] R. Chen, M.G. Christiansen, P. Anikeeva, ACS Nano 7 (2013) 8990–9000.
[16] Madhuri Mandal Goswami, Sci. Rep. 6 (2016) 35721.
[17] D. Sarkar, M. Mandal, J. Phys. Chem. C 116 (5) (2012) 3227–3234.
[18] D. Pal, M. Mandal, A. Chaudhury, B. Das, D. Sarkar, K. Mandal, J. Appl. Phys. 108 (2010) 124317.